information services
gwasanaethau gwybodaeth

1 **Title**

2 Drumming motor sequence training induces apparent myelin remodelling in

3 Huntington's disease: a longitudinal diffusion MRI and quantitative magnetization

4 transfer study

5

6 **Authors**

7 Chiara Casella[1*], Jose Bourbon-Teles[1*], Sonya Bells[2], Elizabeth Coulthard[3], Greg D.

8 Parker[1], Anne Rosser[4,6], Derek K. Jones[1,5], Claudia Metzler-Baddeley[1]

9 *These authors share first authorship

10

11 **Affiliations**

12 [1] Cardiff University Brain Research Imaging Centre (CUBRIC), School of Psychology,

13 Cardiff University, Maindy Road, Cardiff, CF 24 4HQ, UK [2] The Hospital for Sick

14 Children, Neurosciences and Mental Health, Toronto, M5G 1X8, Canada; [3] Clinical

15 Neurosciences, University of Bristol, Bristol, BS10 5NB, UK, [4] School of Biosciences,

16 Cardiff   University,   Museum   Avenue,   Cardiff,   CF10   3AX,   UK.   [5]

17 Mary MacKillop Institute for Health Research, Australian Catholic University,

18 Melbourne, Victoria 3065, Australia.[6] Department of Neurology and Psychological

19 Medicine, Hayden Ellis Building, Maindy Rd, CF24 4HQ

20

21 **Running title**

22 Training-associated myelin-remodelling in HD.

23

24 **Corresponding author**

25 Chiara Casella, CUBRIC, Maindy Road, Cardiff CF24 4 HQ, CasellaC@cardiff.ac.uk.

1. Abstract

Background: Impaired myelination may contribute to Huntington's disease (HD) pathogenesis. **Objective:** This study assessed differences in white matter (WM) microstructure between HD patients and controls, and tested whether drumming training stimulates WM remodelling in HD. Furthermore, it examined whether training-induced microstructural changes are related to improvements in motor and cognitive function. **Methods:** Participants undertook two months of drumming exercises. Working memory and executive function were assessed before and post-training. Changes in WM microstructure were investigated with diffusion tensor magnetic resonance imaging (DT-MRI)-based metrics, the restricted diffusion signal fraction (Fr) from the composite hindered and restricted model of diffusion (CHARMED) and the macromolecular proton fraction (MPF) from quantitative magnetization transfer (qMT) imaging. WM pathways linking putamen and supplementary motor areas (SMA-Putamen), and three segments of the corpus callosum (CCI, CCII, CCIII) were studied using deterministic tractography. Baseline MPF differences between patients and controls were assessed with tract-based spatial statistics (TBSS). **Results:** MPF was reduced in the mid-section of the CC in HD subjects at baseline, while a significantly greater change in MPF was detected in HD patients relative to controls in the CCII, CCIII, and the right SMA-putamen post-training. Further, although patients improved their drumming and executive function performance, such improvements did not correlate with microstructural changes. Increased MPF suggests training-induced myelin changes in HD. **Conclusions:** Though only preliminary and based on a small sample size, these results suggest that tailored behavioural stimulation may lead to neural benefits in early HD, that could be exploited for delaying disease progression.

Key words

Huntington's disease, drumming training, white matter, myelin, diffusion MRI

2. Introduction

2.1 The Pathology of Huntington's disease

Huntington's disease (HD) is a genetic, neurodegenerative disorder caused by an expansion of the CAG repeat within the *huntingtin* gene, leading to debilitating cognitive, psychiatric, and motor symptoms. In addition to striatal grey matter (GM) degeneration [1], HD pathology has been linked to white matter (WM) changes [2–9]. Additionally, an increasing body of research suggests that myelin-associated biological processes at the cellular and molecular level contribute to WM abnormalities [10–15]. Myelin is a multi-layered membrane sheath wrapping axons and is produced by oligodendrocytes. Axon myelination is vital during brain development and critical for healthy brain function [16]. Oligodendrocyte/myelin dysfunction can slow down or stop otherwise fast axonal transport, which in turn can result in synaptic loss and eventually axonal degeneration [17].

2.2 Interventions and Brain Plasticity

As HD is caused by a single-gene, it is an ideal model to study neurodegeneration as a whole, and test for possible beneficial interventions that can slow or suppress disease onset. Despite this, no disease-modifying treatment is approved for patients with HD at present. Recent developments in gene therapy have generated much excitement. However, these have yet to be proved to lead to measurable changes in disease progression [18]. Furthermore, a number of questions linger, for example on the relative strength of different approaches and the possible

3

76 side effects of each therapy [19]. Importantly, these treatments aim to modify and not

77 cure the disease, and while symptomatic therapies for HD are present, and are used

78 for treating chorea and some of the psychiatric symptoms, their effectiveness varies

79 between patients and may lead to clinically significant side-effects [18]. This stresses

80 the need to develop better symptomatic therapies to aid patients and manage HD

81 symptoms.

82   Environmental stimulation and behavioural interventions may have the potential to

83 reduce disease progression and delay disease onset [20–22]. Furthermore, previous

84 studies have detected training-related changes in the WM of both healthy controls

85 [23,24] and patients, including subjects with HD [25]. For example, DT MRI studies

86 have shown microstructural WM changes following balance training in healthy [24] and

87 traumatic brain injury young adults [26]. Other imaging studies have shown DT MRI

88 changes as a result of juggling [27], abacus training [28], extensive piano practice

89 [29,30], working memory training [31], reasoning training [32], and meditation training

90 [33].

91   Converging evidence implicates myelin plasticity as one of the routes by which

92 experience shapes brain structure and function [27,34–38]. Plastic changes in

93 myelination may be implicated in early adaptation and longer-term consolidation and

94 improvement in motor tasks [39–42]. Changes in myelin-producing oligodendrocytes

95 and in GM and WM microstructure have been reported within the first hours of skill

96 acquisition [43,44], implying that experience can be quickly translated into adaptive

97 changes in the brain.

98   This study assessed whether two months of drumming training, involving

99 practising drumming patterns in ascending order of difficulty, could trigger WM

100 microstructural changes, and potentially myelin remodelling, in individuals with HD.

101 Specifically, we hypothesised that changes in *microstructural* metrics would be more

102 marked in patients than in healthy subjects, based on reports of larger training-

103 associated changes in structural MRI metrics in patient populations than in healthy

104 controls [34].

105 The drumming intervention was designed to target cognitive and motor

106 functions known to be mediated by cortico-basal ganglia loops. More specifically the

107 training focused on the learning of novel motor sequences and their rhythm and timing,

108 engaging executive processes known to be impaired in HD [45]. These included

109 focused attention (e.g. paying attention to the drumming sequence), multi-tasking

110 attention (e.g. listening and movement execution), movement-switching (e.g.

111 switching between dominant and non-dominant hand) and response speed [25]. At the

112 anatomical level, attention and executive functions rely on cortico-basal ganglia loops

113 involving the striatum, which also plays a fundamental role in motor control and motor

114 learning [46,47]. This shared reliance on overlapping cortico-basal ganglia networks

115 may contribute to the beneficial effects of physical exercise on executive functioning

116 in healthy older adults [48], and in patients with Parkinson's disease [49]. Additionally,

117 in a previous pilot study assessing the feasibility of the present drumming training, we

118 observed WM changes and improvements in executive functions in HD patients

119 following the intervention [25].

120 Previous WM plasticity neuroimaging studies [27,50] have predominantly

121 employed indices from diffusion tensor MRI (DT-MRI) [51]. However, while sensitive,

122 such measures are not specific to changes in specific sub-compartments of WM

123 microstructure, challenging the interpretation of any observed change in DT-MRI

124 indices [52,53]. To improve compartmental specificity beyond DT-MRI, the present

125 study explored changes in the macromolecular proton fraction (MPF) from quantitative

126 magnetization transfer (qMT) [54] imaging and the restricted diffusion signal fraction

127 (Fr) from the composite hindered and restricted model of diffusion (CHARMED) [55].

128 Fractional anisotropy (FA) and radial diffusivity (RD) from DT-MRI [51] were included

129 for comparability with previous training studies [27,56,57].

130   The MPF has been proposed as a proxy MRI marker of myelin [58].

131 Accordingly, histology studies show that this measure reflects demyelination

132 accurately in Shiverer mice [59], is sensitive to de-myelination in multiple sclerosis

133 patients [60] and reflects WM myelin content in post-mortem studies of multiple

134 sclerosis brains [61]. Fr, on the other hand, represents the fraction of signal-

135 attenuation that can be attributed to restricted diffusion, which is presumed to be

136 predominantly intra-axonal, and therefore provides a proxy measure of axonal density

137 [62].

138   Training effects were investigated in WM pathways linking the putamen and the

139 supplementary motor area (SMA-Putamen), and within three segments of the corpus

140 callosum (CCI, CCII, CCIII). The SMA has efferent and afferent projections to the

141 primary motor cortex and is involved in movement execution, and previous work has

142 reported altered DT-MRI metrics in the putamen-motor tracts of symptomatic HD

143 patients [63]. The anterior and anterior-mid sections of the corpus callosum contain

144 fibres connecting the motor, premotor and supplementary motor areas in each

145 hemisphere [64]. Previous work has demonstrated a thinning of the corpus callosum

146 in post-mortem HD brains [65], altered callosal DT-MRI metrics in both pre-

147 symptomatic and symptomatic HD patients [66,67], and a correlation between these

148 metrics and performance on motor function tests [68]. Given previous reports of an

149 effect of motor learning on myelin plasticity [38], we expected changes following

150 training to be more marked in MPF, as compared to the other non-myelin sensitive

metrics assessed in this study. We also investigated the relationship between training-associated changes in MRI measures, and changes in drumming performance and cognitive/executive function. Finally, as previous evidence has shown widespread reductions in MPF in premanifest and manifest HD patients [69], we used tract-based spatial statistics (TBSS) [70] to investigate patient-control differences in MPF before training, across the whole brain; this aided the interpretation of the post-training microstructure changes we detected.

3. Materials and Methods

3.1 Participants

The study was approved by the local National Health Service (NHS) Research Ethics Committee (Wales REC 1 13/WA/0326) and all participants provided written informed consent. All subjects were drumming novices and none had taken part in our previously-reported pilot study [25]. Fifteen HD patients were recruited from HD clinics in Cardiff and Bristol. Genetic testing confirmed the presence of the mutant huntingtin allele. Thirteen age, sex, and education-matched healthy controls were recruited from the School of Psychology community panel at Cardiff University and from patients' spouses, carers or family members. The inclusion criteria were the following: no history of head injury, stroke, cerebral haemorrhages or any other neurological condition; eligible for MRI scanning; stable medication for at least four weeks prior to the study.

Of the recruited sample, two patients were not MRI compatible, four withdrew during the study and one patient's MRI data had to be excluded due to excessive motion. Therefore, while drumming performance and cognitive data from 11 patients were assessed, only 8 patients had a complete MRI dataset. One control participant

176 was excluded due to an incidental MRI finding, two participants dropped out of the

177 study and a fourth participant was not eligible for MRI. In total, we assessed drumming

178 and cognitive tests performance in 8 controls, while MRI data from nine controls were

179 available for analyses. Table 1 summarizes patients demographic and background

180 clinical characteristics. Most patients were at early disease stages, however two were

181 more advanced, as shown by their Total Motor Score (TMS; 69 and 40, respectively)

182 and Functional Assessment Score (FAS; 18 and 17, respectively). Table 2

183 summarizes demographic variables and performance in the Montreal Cognitive

184 Assessment (MoCA) [71] and in the revised National Adult Reading Test (NART-R)

185 (Nelson, 1991) for patients and controls. While the groups did not differ significantly in

186 age, controls were on average slightly older, performed significantly better on the

187 MoCA, and had a significantly higher NART-IQ than patients.

188

189 ### 3.2 Training intervention: Drumming-based rhythm exercises

190   The rhythm exercise and drumming training previously described in [25] was

191 applied. Participants were provided with twenty-two 15 min training sessions on CDs,

192 a pair of Bongo drums and a drumming diary and could practise at home. They were

193 asked to exercise for 15 min per day, 5 times per week, for 2 months and to record the

194 date and time of each exercise in their diary. Each training session introduced a

195 drumming pattern based on one of the following rhythms: Brazilian samba, Spanish

196 rumba, West-African kuku and Cuban son. After a brief warm up, trainees were

197 encouraged to drum along with the instructor, initially with each hand separately and

198 then with both hands alternating, starting with the dominant hand first and then

199 reversing the order of the hands. The first exercises were based on very simple, slow,

8

200 and regular patterns but the level of complexity and speed increased over the training

201 sessions.

202   Importantly, each individual progressed through the training adaptively at their

203 own pace i.e., as long as they exercised for the specified time, they could repeat each

204 session as often as they felt necessary to master it. To maintain engagement and

205 motivation, the training incorporated pieces of music based on rhythms participants

206 had learned and could drum along to. The researcher (JBT) supervised the first

207 training sessions and then remained in regular telephone contact (at least once a

208 week) with each participant throughout the intervention. Whenever possible, carers

209 and/or spouses were involved in the study to support the training. Control participants

210 started with Session 3 since the first two exercises were built on a very low level of

211 complexity, with slow, regular patterns of movement required. Patients, on the other

212 hand, started with simpler exercises, but could progress to the following sessions

213 whenever they felt comfortable.

214

215
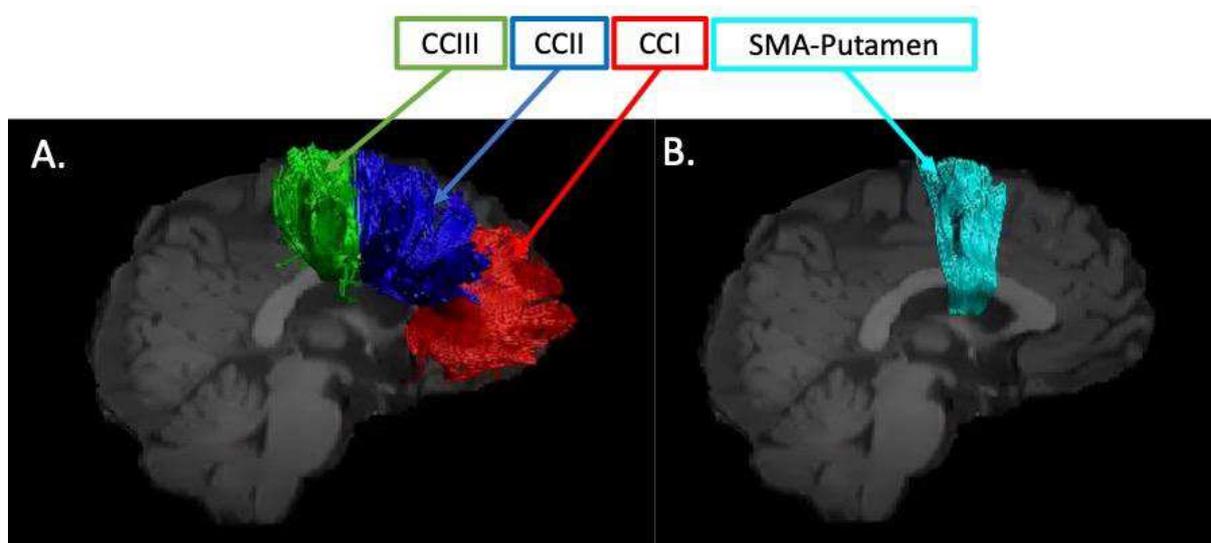
216

217 *Figure 1.*

218

219

3.3 Drumming assessment

Progress in drumming ability was assessed by digitally recording participants' drumming performance for three patterns of ascending levels of difficulty (easy, medium and hard), which were not part of the training sessions, at baseline and after the training. Each recording was judged by an independent rater, blind to group and time, according to an adopted version of the Trinity College London marking criteria for percussion (2016) (www.trinitycollege.com).

3.4 Cognitive assessments

Different aspects of cognition and executive function were assessed before and after the training as previously described [25]. Multi-tasking was assessed with a dual task requiring simultaneous box crossing and digit sequences repetition [73]. Attention switching was assessed with the trails test (VT) requiring the verbal generation of letter and digit sequences in alternate order relative to a baseline condition of generating letter or digit sequences only (69). Distractor suppression was tested with the Stroop task involving the naming of incongruent ink colours of colour words. Verbal and category fluency were tested using the letter cues "F", "A", "S" and "M", "C", "R" as well as the categories of "animals" and "boys' names" and "supermarket items" and "girls' names" respectively [74]. In total, we assessed 7 outcome variables, and percentage change scores in performance were computed for each of these variables (Table 3).

3.5 MRI data acquisition

242   MRI data were acquired on a 3 Tesla General Electric HDx MRI system (GE

243   Medical Systems, Milwaukee) using an eight channel receive-only head RF coil at the

244   Cardiff University Brain Research Imaging Centre (CUBRIC). The MRI protocol

245   comprised the following images sequences: a high-resolution fast spoiled gradient

246   echo (FSPGR) T_1-weighted (T_1-w) sequence for registration; a diffusion-weighted

247   spin-echo echo-planar sequence (SE\EPI) with 60 uniformly distributed directions

248   (b = 1200 s/mm^2), according to an optimized gradient vector scheme [75]; a

249   CHARMED acquisition with 45 gradient orientations distributed on 8 shells (maximum

250   b-value = 8700s/mm^2) [55]; and a 3D MT-weighted fast spoiled gradient recalled-echo

251   (FSPGR) sequence [76]. The acquisition parameters of all scan sequences are

252   reported in Table 4. Diffusion data acquisition was peripherally gated to the cardiac

253   cycle. The off-resonance irradiation frequencies (Θ) and their corresponding

254   saturation pulse amplitude (ΔSAT) for the 11 Magnetization transfer (MT) weighted

255   images were optimized using Cramer-Rao lower bound optimization [76].

256

257   **_3.6 MRI data processing_**

258   The diffusion-weighted data were corrected for distortions induced by the

259   diffusion-weighted gradients, artefacts due to head motion and EPI-induced

260   geometrical distortions by registering each image volume to the T_1-w anatomical

261   images [77], with appropriate reorientation of the encoding vectors [78], all done in

262   ExploreDTI (Version 4.8.3) [79]. A two-compartment model was fitted to derive maps

263   of FA and RD in each voxel [80]. CHARMED data were corrected for motion and

264   distortion artefacts according to the extrapolation method of [81] The number of

265   distinct fiber populations (1, 2, or 3) in each voxel was obtained using a model selection

266   approach [52], and Fr was calculated per voxel with an in-house software [52] coded

267 in MATLAB (The MathWorks, Natick, MA). MT-weighted SPGR volumes for each

268 participant were co-registered to the MT-volume with the most contrast using an affine

269 (12 degrees of freedom, mutual information) registration to correct for inter-scan

270 motion using Elastix [82]. The 11 MT-weighted SPGR images and T_1 map were

271 modelled by the two pool Ramani's pulsed MT approximation [83,84], which included

272 corrections for amplitude of B_0 field inhomogeneities. This approximation provided

273 MPF maps, which were nonlinearly warped to the T_1-w images using the MT-volume

274 with the most contrast as a reference using Elastix (normalized mutual information

275 cost function) [82].

276

277 ***3.7 Deterministic Tractography***

278   Training-related changes in FA, RD, Fr, and MPF were quantified using a

279 tractography approach in pathways interconnecting the putamen and the

280 supplementary motor area bilaterally (SMA-Putamen), and within three segments of

281 the corpus callosum (CCI, CCII and CCIII) [64] (Figure 1).

282   Whole brain tractography was performed for each participant in their native

283 space using the damped Richardson-Lucy algorithm [85], which allows the recovery

284 of multiple fiber orientations within each voxel including those affected by partial

285 volume. The tracking algorithm estimated peaks in the fiber orientation density function

286 (fODF) by selecting seed points at the vertices of a 2×2×2 mm grid superimposed over

287 the image and propagated in 0.5-mm steps along these axes re-estimating the fODF

288 peaks at each new location [86]. Tracks were terminated if the fODF threshold fell

289 below 0.05 or the direction of pathways changed through an angle greater than 45°

290 between successive 0.5 mm steps. This procedure was then repeated by tracking in

291 the opposite direction from the initial seed-points.

292   The WM tracts of interest were extracted from the whole-brain tractograms by

293   applying way-point regions of interest (ROI) [87]. These were drawn manually by one

294   operator (JBT) blind to the identity of each dataset on color-coded fiber orientation

295   maps in native space guided by the following anatomical landmark protocols (Figure

296   2).

297   3.7.1 Corpus callosum

298   Reconstruction of the CC segments followed the protocol of Hofer and Frahm

299   [64] as illustrated in Figure 2A. Segment reconstructions were visually inspected and,

300   if necessary, additional gates were placed to exclude streamlines inconsistent with the

301   known anatomy of the CC.

302   3.7.2 SMA-putamen pathway

303   One axial way-point ROI was placed around the putamen and one axial ROI

304   around the supplementary motor cortex [88] (Figure 2B). A way-point gate to exclude

305   fibres projecting to the brain stem was placed inferior to the putamen.

306

307
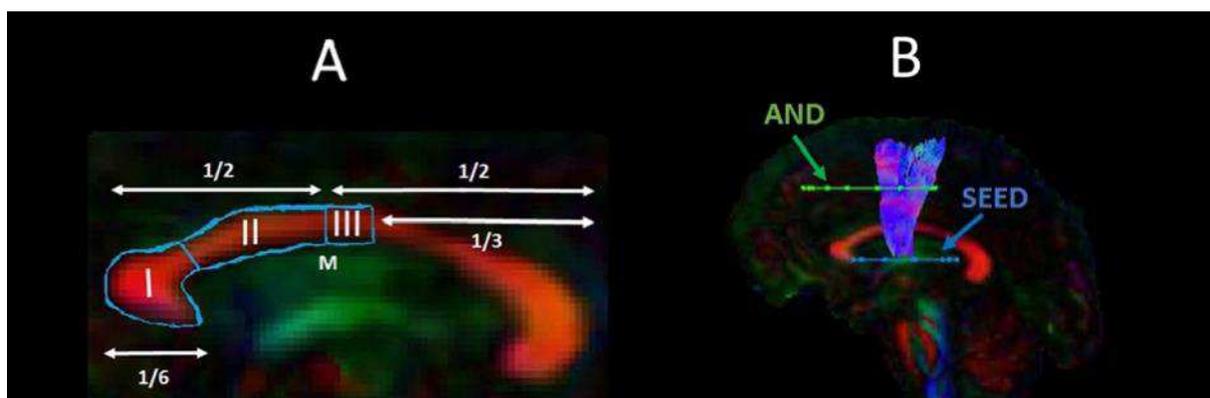
308

309   *Figure 2.*

310

311

3.8 Statistical analyses

313   Statistical analyses were carried out in R Statistical Software (Foundation for

314 Statistical Computing, Vienna, Austria).

315 3.8.1 Assessment of training effects on drumming performance

316   Improvements in drumming performance were analysed with a two-way mixed

317 analysis of variance (ANOVA) testing for the effects of group (HD/controls), time of

318 assessment (before/after the training) and group by time interaction effects. We also

319 confirmed detected effects to the ones obtained by running a robust mixed ANOVA,

320 using the bwtrim R function from the WRS2 package [89]. This implements robust

321 methods for statistical estimation and therefore provides a good option to deal with

322 data presenting small sample sizes, skewed distributions and outliers [90]. Significant

323 effects were further explored with post-hoc paired and independent t-tests. The

324 reliability of the post-hoc analyses was assessed with bootstrap analysis based on

325 1000 samples and the 95% confidence interval (CI) of the mean difference is provided

326 for each significant comparison.

327 3.8.2 Assessment of group differences in the effect of training on cognitive

328 performance

329   Performance measures in executive function tasks have been shown to share

330 underlying cognitive structures [91]. Therefore, PCA was employed to reduce the

331 complexity of the cognitive data and hence the problem of multiple comparisons as

332 well as to increase experimental power. PCA was run on change scores for all

333 participants across both groups. Due to the relatively small sample size, we first

334 confirmed with the Kaiser-Meyer-Olkin (KMO) test that our data was suited for PCA.

335 Subsequently, we followed guidelines to limit the number of extracted components

336 [92,93], as follows: first, we employed the Kaiser criterion of including all components

337 with an eigenvalue greater than 1; second, we inspected the Cattell scree plot [94] to

338 identify the minimal number of components that accounted for most variability in the

339 data; third, we assessed each component's interpretability. A PCA procedure with

340 orthogonal Varimax rotation of the component matrix was used. Loadings that

341 exceeded a value of 0.5 were considered as significant.

342   Next, we assessed group differences in the component scores with permutation

343 analyses, to understand whether the training had differentially affected HD patients as

344 compared to controls. Permutation testing relies only on minimal assumptions and can

345 therefore be applied when the assumptions of a parametric approach are untenable

346 such as in the case of small sample sizes. Significant group differences were tested

347 using 5,000 permutations and the effect sizes of significant differences were assessed

348 with Cohen's d [95]. Multiple comparison correction was based on a 5% false

349 discovery rate (FDR) using the Benjamini-Hochberg procedure [96].

350 3.8.3 Training effects on WM microstructure

351   Median measures of FA, RD, Fr and MPF were derived for each of the

352 reconstructed tracts in ExploreDTI [79]. A percentage change score in these measures

353 between baseline and post-training was calculated in each tract (CCI, CCII, CCIII, left

354 and right SMA-Putamen).

355   Previous research has shown that variation in the microstructural properties of

356 WM may represent a global effect, rather than being specific to individual tracts, and

357 that WM measures are highly correlated across WM areas [56,97,98]. Therefore, we

358 inspected the inter-tract correlation for each of microstructural metric and found that

359 MPF values were highly correlated, whereas this was not true for the other metrics

360 (Figure 3). Hence, percentage change scores in MPF across the different tracts were

361 transformed with PCA to extract meaningful anatomical properties, following the

procedure described above for the PCA of cognitive change scores. PC scores for each participant were then used as dependent variables in a permutation-based analysis using 5,000 permutations to assess group differences in training associated changes in MPF. Finally, as a post-hoc exploration, we looked for between-groups differences in MPF changes in the individual tracts using 5000 permutations.

Training-associated changes in FA, Fr and RD were investigated with permutation analyses separately for each tract. Significant group differences in these measures were tested using 5,000 permutations. Multiple comparison correction was based on a 5% FDR using the Benjamini-Hochberg procedure [96]. Cohen's d [95] was used to assess the effect size for those changes found to be significant.

3.8.4 Training effects on WM microstructure

TBSS [70] was carried out to investigate baseline differences in MPF between HD subjects and healthy controls, , to gain a better insight into differences in training-associated changes. To produce significance maps, a voxel-wise analysis was performed on the MPF projected 4D data for all voxels with FA ≥ 0.20 to exclude peripheral tracts where significant inter-subject variability exists. Inference based on permutations (5,000 permutations) and threshold-free-cluster-enhancement was used. The significance level was set at $p < 0.05$ and corrected by multiple comparisons (family-wise error, FWE).

3.8.5 Relationship between changes in MRI measures and changes in drumming and cognitive performance

We computed percentage change scores for the drumming performance, in the same way cognitive change scores were calculated. Scores were computed for the easy test pattern in patients and for the medium test pattern in controls, as these training patterns showed a significant improvement in the two groups, respectively.

387   Spearman correlation coefficients were calculated between drumming and cognitive

388   performance, and microstructural components that showed significant group

389   differences, to assess whether microstructural changes were related to any drumming

390   and/or cognitive benefits of the training.

391   3.8.6 Exploration of the possible confounding effects of differences in training-

392   compliance and IQ

393   We examined the training diaries of each participant to assess compliance with

394   training. Each session was marked as completed if the whole 15 minute session had

395   been carried out. Each participant was assigned a score representing the number of

396   training sessions they performed (e.g. a score of 40 if 40 sessions had been carried

397   out). We then assessed group differences with permutation analyses, to test whether

398   there was a significant difference in the amount of training sessions carried out by the

399   groups, and hence understand whether this variable had to be accounted for in the

400   analysis. Significant group differences were tested using 5,000 permutations.

401   Finally, as there was a significant difference in IQ between patients and controls

402   (Table 2), we investigated whether any training-associated change might be due to

403   differences in premorbid intelligence. The sample size of this experiment was very

404   small, and therefore it was not possible to perform a multiple regression or an analysis

405   of covariance (ANCOVA), to understand the possible influence of IQ as confounding

406   variable. Accordingly, the statistical power to establish the incremental validity of a

407   covariate in explaining an outcome has been shown to be extremely low, and therefore

408   to require large sample sizes [99]. As a potential solution to this issue, we instead

409   performed separate non-parametric Spearman correlation analyses between NART-

410   IQ scores (as this test showed the largest difference between groups), and MRI and

411   cognitive measures showing significant training effects; this allowed us to gain some

412 insight into whether there was a significant association between premorbid intelligence

413 and training-associated changes.

414

415

416 **4. Results**

417 **4.1 Training effects on drumming performance**

418 The mixed ANOVA of drumming performance for the easy and medium test

419 pattern showed a significant effect of group [easy: $F(1,17) = 22.3$, $p < 0.001$; medium:

420 $F(1,17) = 13.1$, $p = 0.002$] and time [easy: $F(1,17) = 12.83$, $p = 0.004$; medium: $F(1,17)$

421 $= 13.4$, $p = 0.002$] but no interaction (easy: $p = 0.8$; medium: $p = 0.3$). For the hard test

422 pattern there was only a significant effect of group [$F(1,17) = 9.95$, $p = 0.006$] but not

423 of time ($p = 0.1$) and there was no interaction ($p = 0.4$). Results from the robust mixed

424 ANOVA were largely consistent with the above. Specifically, the easy and medium test

425 patterns showed a significant effect of group (easy: $p = 0.002$; medium: $p = 0.02$) and

426 time (easy: $p = 0.04$; medium: $p = 0.049$) but no interaction (easy: $p = 0.45$; medium:

427 $p = 0.69$). The hard test pattern showed a significant effect of group ($p = 0.02$) but not

428 of time ($p = 0.22$) and no interaction ($p = 0.8$). Figure 4 summarises the average

429 drumming performance per group and time point. Overall patients' drumming

430 performance was poorer than controls. Patients improved their drumming

431 performance significantly for the easy pattern [$t(10) = 2.7$, $p = 0.02$; 95% CI of mean

432 difference: $1.5 – 7.8$] and controls for the medium pattern [$t(7) = 3.8$, $p = 0.01$; 95% CI

433 of mean difference: $2.8 – 8.5$].

434

435 **4.2 Group differences in the effect of training on cognitive performance**

436   Three components, accounting for 79% of the variance in performance

437   improvement in the cognitive benchmark tests, were extracted. The first component

438   loaded highly on performance changes in the dual task (total number of boxes

439   identified under dual task condition), the Stroop task (Stroop interference score), and

440   the trails making task (Trail test switching). Since these variables all measure

441   executive functions including focused attention and distractor suppression, the first

442   component was labelled "executive" component. The second component loaded on

443   variables reflecting the ability to correctly recall digits sequences (i.e. number of

444   correct digits recalled under single and dual task condition) and was therefore labelled

445   "working memory capacity" component. Finally, the third extracted component loaded

446   highly on verbal and category fluency and was therefore labelled "fluency" component

447   (Table 5).

448   We tested whether the two groups differed in terms of post-training cognition

449   changes, by running permutation analyses on the individual scores for the three

450   extracted components. The two groups differed in the executive component ($t = -1.03$,

451    $p = 0.008$, FDR-corrected $p = 0.024$, $d = 1.15$). However, no significant group

452   differences were detected in the other two components (Working Memory capacity: t

453    $= -0.22$, $p = 0.3296$, FDR-corrected $p = 0.3296$; Fluency: $t = -0.39$, $p = 0.242$ FDR

454   corrected $p = 0.3296$).

455

456   **4.3 Training effects on WM microstructure**

457   Table 6 reports a summary of the training associated changes in FA, RD, Fr

458   and MPF, across the different tracts.

459   4.3.1 Training-associated group differences in FA

460   Permutation analyses of FA changes across the different tracts revealed no

461   significant differences between HD and control groups [CCI: t = 1.22, p = 0.91 (FDR-

462   corrected); CCII: t = 2.65, p = 0.91 (FDR-corrected); CCIII: t = 0.325, p = 0.13 (FDR-

463   corrected); right SMA-Putamen: t = -9.54, p = 0.10 (FDR-corrected); left SMA-

464   Putamen: t = 5.16, p = 0.77 (FDR-corrected).

465   4.3.2 Training-associated group differences in RD

466   There were no significant differences in RD changes following training

467   between HD patients and controls [CCI: t = -0.48, p = 0.45 (FDR-corrected); CCII: t =

468   -1.29, p = 0.45 (FDM-corrected); CCIII: t = -1.04, p = 0.45 (FDR-corrected); right SMA-

469   Putamen, t = 4.01 , p = 0.81 (FDR-corrected); left SMA-Putamen, t = -3.68, p = 0.39

470   (FDR-corrected).

471   4.3.3 Training-associated group differences in Fr

472   Permutation analyses of Fr changes across the different tracts revealed no

473   significant differences between HD and control groups [CCI: t = 3.39, p = 0.82 (FDR-

474   corrected; CCII: t = -0.17, p = 0.82 FDR-corrected; CCIII: t = 3.08, p = 0.82 (FDR-

475   corrected); right SMA-Putamen: t = -5.24, p = 0.82 (FDR-corrected); left SMA-

476   Putamen: t = 1.05, p = 0.82 (FDR-corrected)].

477   4.3.4 Training-associated group differences in MPF

478   PCA of change scores in MPF revealed one single component explaining

479   70.2% of the variance. This component presented high loadings from all the tracts

480   investigated. A significant group difference was found for the MPF change-score

481   component, indicating that HD patients presented significantly greater MPF changes

482   in response to training, as compared to controls [t(14) = -1.743, n = 17, p = 0.03, d =

483   1.796].

484   Finally, we found a significant difference in mean MPF change scores between

485   the two groups for CCII [$t(14)$ = -20.72, p = 0.04, d = 0.93], CCIII [$t(14)$ = -25.87, p =

486   0.04, d = 1.07], and the right SMA-putamen pathway [$t(14)$ = -25.48, p = 0.04, d = 1.15]

487   after FDR correction, therefore indicating that there was a differential group effect of

488   training on MPF within these tracts (Figure 5).

489

490

491

492

21
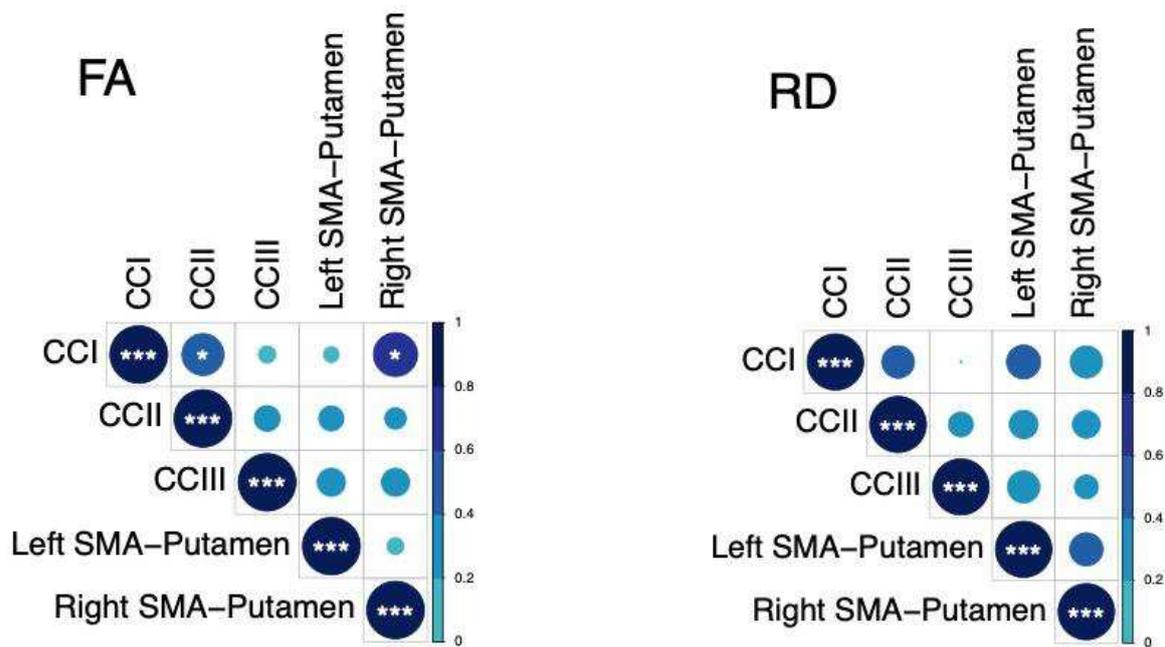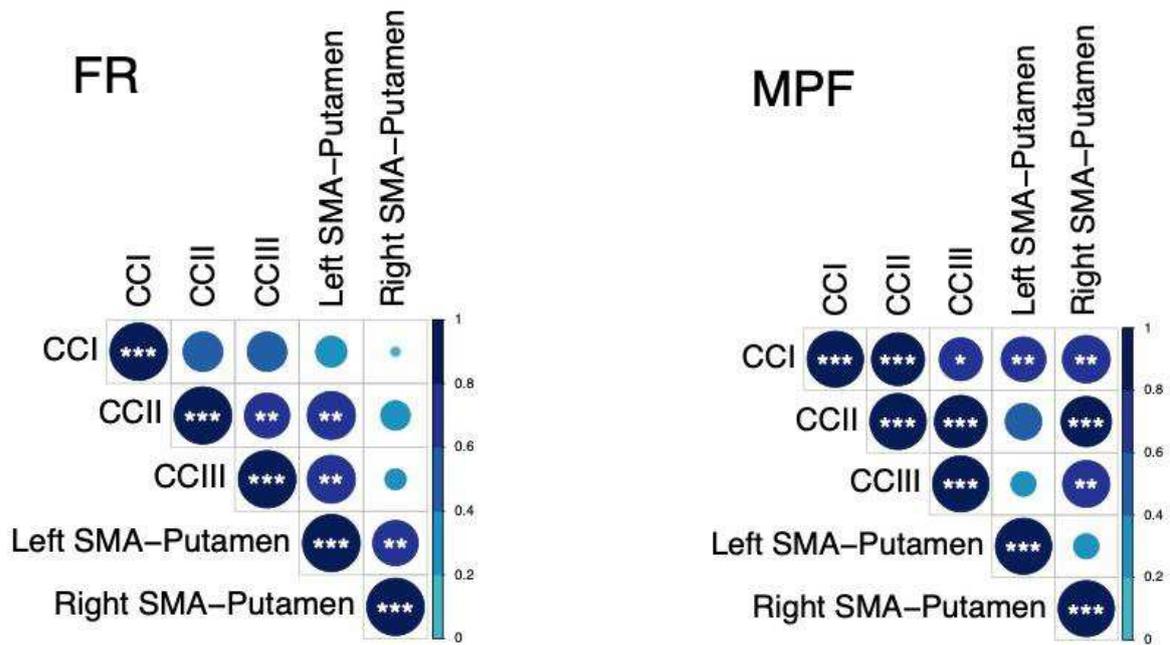
Figure 3.

4.4 Relationship between training-associated changes in MRI measures, and changes in drumming and cognitive performance.

We did not find a significant association between the 'MPF' component scores and improvement in drumming performance (PC1: rho = -0.14, p > 0.05). Moreover, although no significant correlation was observed between the 'Executive' and the 'MPF' component scores, there was a positive trend (rho = .348, p = .171).

4.5 Baseline differences in MPF

Baseline MPF was reduced in the HD group compared to controls, in the midbody of the CC (t = 3.13, p = .05, FWE corrected). Figure 6 shows the areas with reduced MPF in HD patients, in blue.

HD PATIENTS (N=8) CONTROLS (N=7)
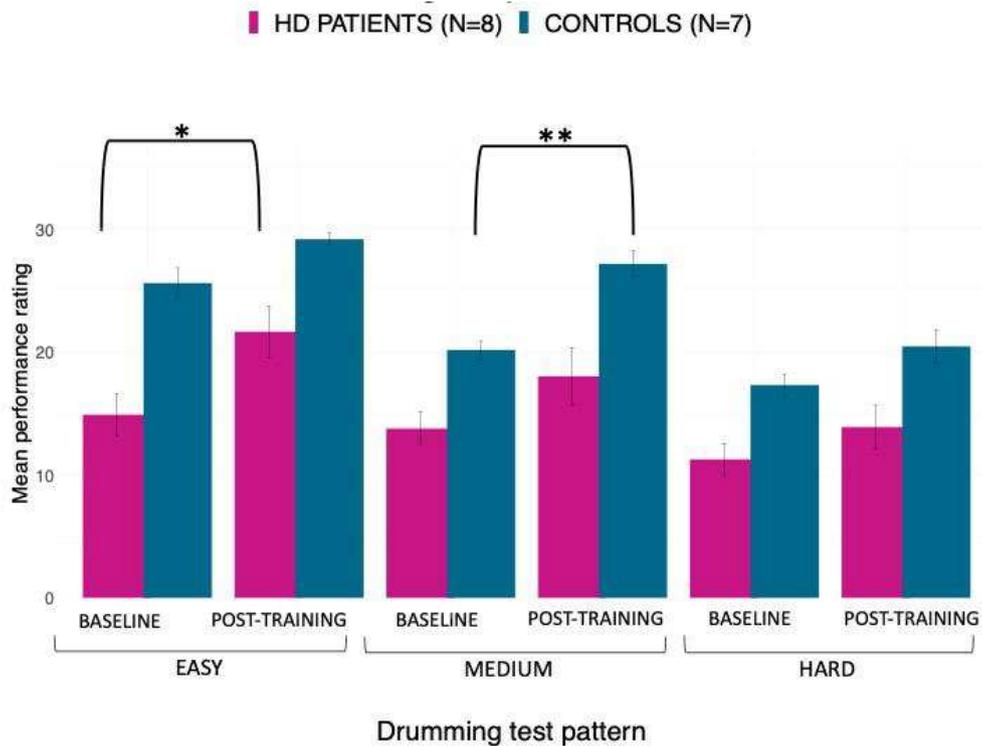
509

510 *Figure 4.*

511

512

513 **4.6.   *Exploration* of the possible confounding effects of differences in training-**

514 **compliance and IQ**

515   The permutation analysis of training compliance revealed that there was not a

516 significant difference in the number of training sessions between HD patients (mean =

517 38.1, SD = 4.2) and healthy controls (mean = 39.6, SD = 1.2), $t = 1.45$, $p = 0.76$.

518 Therefore, the total time spent training should not have influenced any training-

519 associated change in microstructure and/or cognitive measures. Furthermore, we did

520 not detect a significant association of participants' NART-IQ scores with 'MPF'

521 component scores (rho = -0.4, $p = 0.10$), nor with 'Executive' component scores (rho

522 = -0.34, $p = 0.18$), suggesting that premorbid intelligence should not have had an

523 influence on training-associated effects.

524

5. Discussion

Based on evidence that myelin impairment contributes to WM damage in HD [3], and the suggestion that myelin plasticity underlies the learning of new motor skills [27,38], the present study explored whether two months of drumming training would result in changes in WM microstructure in HD patients. Specifically, we expected to detect changes in MPF, as marker of WM myelin plasticity, in HD patients relative to healthy controls.

Firstly, we demonstrated a behavioural effect of the training by showing a significant improvement in drumming performance in patients (easy test pattern) and controls (medium test pattern). We did not detect any group differences in training-associated changes in the diffusion based indices of FA, RD and Fr. However, as hypothesised, we found a group difference in training-induced changes in the MPF PCA component. Specifically, HD patients showed significantly higher increases in MPF relative to controls. Furthermore, through exploratory post-hoc investigations, we detected significantly higher training-induced MPF changes within the CCII, CCIII and the right SMA-putamen pathway between patients and controls. Additionally, TBSS analysis of baseline differences in MPF suggested partial overlap of WM areas showing significant MPF reductions at baseline with areas showing changes post-training (i.e. CCII and CCIII).

MPF can be affected by inflammation [100] and in advanced HD it is likely that inflammation goes hand-in-hand with myelin breakdown [101]. However, a recent CSF biomarker study found no evidence of neuro-inflammation in early-manifest HD [102]. Furthermore, recent evidence shows that this measure may be inconsistent when investigated in relatively small WM areas, presumably because of the effect of spatial heterogeneity in myelin thickness [103]. Nevertheless, the within-subjects design

550 employed in the present study should have helped to minimise noise due to the spatial

551 inconsistency of this measure. Therefore, though preliminary and based on a small

552 sample size, these findings suggest that two months of drumming and rhythm

553 exercises may result in myelin remodelling in patients with early HD.

554   It is plausible that this group difference arose due to WM microstructural

555 differences between patients and controls before the training. Accordingly, the HD

556 group showed a significantly lower baseline MPF, consistent with lower myelin content

557 [3]. Furthermore, previous studies have reported that training-associated percentage

558 changes in MRI measures tend to be higher in patients than in healthy subjects [34].

559 One possibility is that in the healthy brain, neural networks may be optimally

560 myelinated, and further increasing myelin may not improve performance [104–106].

561 Hence, the MPF changes in patients relative to controls might depict mainly a 'catch-

562 up effect' to the better baseline status of the control group. However, disentangling the

563 impact of prior WM microstructural differences on microstructural plasticity during

564 learning is beyond the scope of the current work.

565   Notably, the behavioral effect of drumming training and cognition differed

566 between patients and controls. Patients improved in the easy drumming test pattern,

567 and controls improved in the medium test pattern. Furthermore, consistent with

568 evidence from our pilot study [25], patients showed increases in the executive function

569 components whilst control participants did not show improvements in their cognition.

570 Therefore, inter-group differences in microstructural changes might not only be due to

571 baseline WM microstructural differences, but also to a different behavioral effect of the

572 task between HD subjects and controls. For instance, control participants performed

573 close to ceiling in the easy test pattern, and as the training was tailored to patients'

574 needs, some of the earlier practice sessions may not have optimally challenged them.

575 The fact that the training seemed more taxing for patients than controls may also

576 explain why improvements in executive functions and changes in MPF were only

577 observed for the patients. Interestingly, baseline IQ was significantly different between

578 the two groups, and this might have had some influence on training performance and

579 on training-associated effects. Here, we failed to find an association between IQ

580 scores and changes in MRI and cognitive measures. However, future studies with

581 larger sample sizes might allow to utilize more advanced statistical approaches, such

582 as an ANCOVA, to better model the possible influence of premorbid IQ on training

583 effects, both at the neural and cognitive level.

584 A critical question relevant to all training studies concerns the functional

585 significance of any observed neural changes. If, and to what degree adaptive

586 alterations in myelin content can facilitate behavioural change remains poorly

587 understood [105]. In the present study, no significant relationships between changes

588 in MRI measures and changes in drumming proficiency or performance in cognitive

589 tests were found. This might have been due to non-specific training-related neural

590 responses. Specifically, while the training exercise might have triggered changes in

591 brain structure, training-induced changes may not necessarily co-vary with

592 improvements in performance. Alternatively, it might be that the study was

593 insufficiently powered to detect brain-function correlations. The minimum sample size

594 required to detect a correlation was calculated to be 64 people ($\alpha = 0.05$; 80% power;

595 medium effect size; GPower 3 software). Therefore, these results need replication in

596 larger samples. A lack of correlation between structural and functional changes after

597 training has been reported in other studies (including well-powered studies) and may

598 suggest that these processes follow different time courses and/or may occur in

599 different brain regions [107].

600   It is important to note that our study did not include a non-intervention patient

601   group. Within the 12 month time period of this study it was not possible to recruit a

602   sufficiently large number of well-matched patient controls. Therefore, we cannot

603   disentangle the effects of the training on WM microstructure from HD-associated

604   pathological changes. However, given that HD is a progressive neurodegenerative

605   disease associated with demyelination [3], it is unlikely that increases in MPF observed

606   in the patient group were due to the disease itself. Finally, while the majority of training

607   studies assess brain structural changes between baseline and post-training [34],

608   presumably on account of cost and participant compliance, we suggest that acquiring

609   intermittent scans during the training period could have helped to better capture and

610   understand changes in WM microstructure observed in this study. Accordingly, future

611   studies might be able to provide greater insights into the complex nonlinear

612   relationships between structural changes and behaviour [108].

613   To conclude, we have demonstrated that two months of drumming and rhythm

614   exercises result in a significantly greater change in a proxy MRI measure of myelin in

615   patients with HD relative to healthy controls. Whilst the current results require

616   replication in a larger patient group with an appropriately matched patient control

617   group, they suggest that behavioural stimulation may result in neural benefits in HD

618   that could be exploited for future therapeutics aiming to delay disease progression.

619

620

A.

B.

C.

Variables factor map (PCA)

D.

HD PATIENTS (N=8)   CONTROLS (N=7)
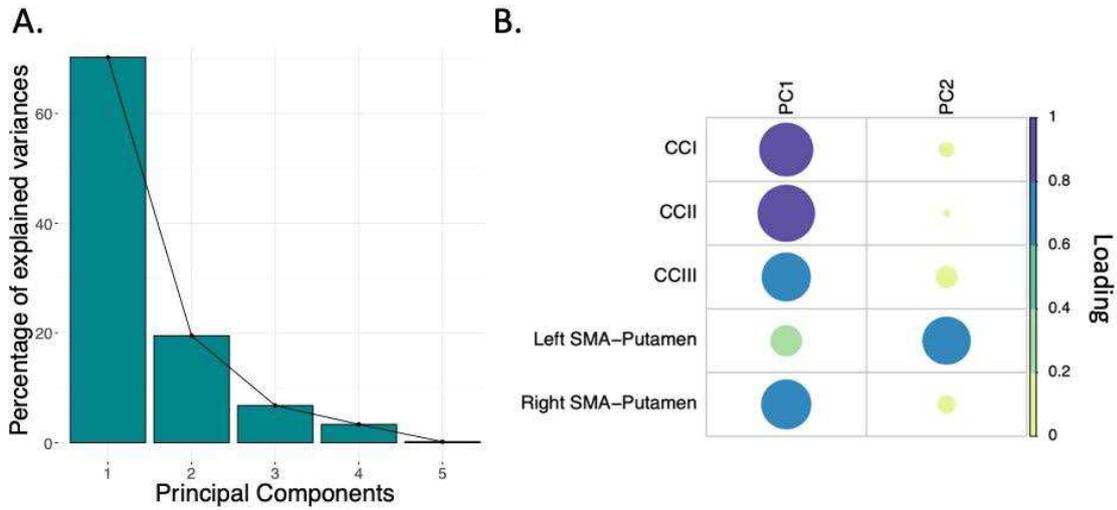
621
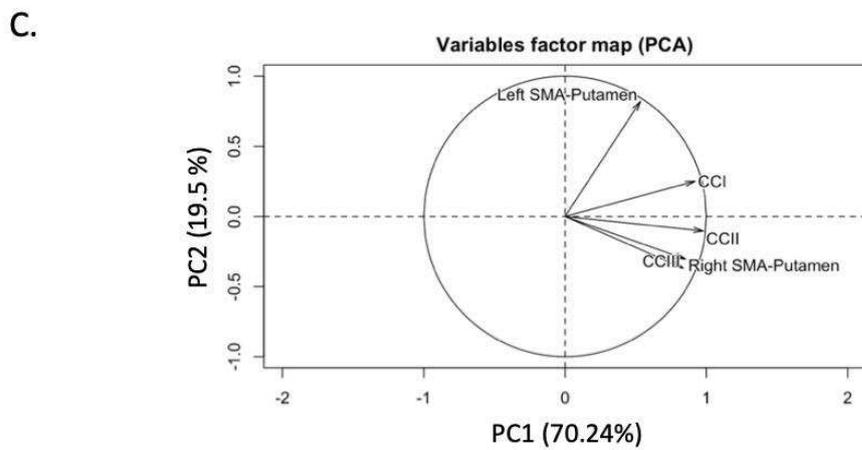
622

623

624   *Figure 5.*

625

626

28

Figure 6.

29

References

645

646   [1]   Weaver KE, Richards TL, Liang O, Laurino MY, Samii A, Aylward EH. Longitudinal

647   diffusion tensor imaging in Huntington's Disease. Exp Neurol 2009;216:525–9.

648   https://doi.org/10.1016/j.expneurol.2008.12.026.

649   [2]   Bardile CF, Garcia-Miralles M, Caron N, Langley S, Teo RTY, Petretto E, et al. A43

650   Intrinsic mutant HTT-mediated defects in oligodendroglia cells contribute to myelin

651   deficits and behavioural abnormalities in huntington disease. J Neurol Neurosurg

652   Psychiatry 2018;89:A15–6. https://doi.org/10.1136/jnnp-2018-EHDN.41.

653   [3]   Bartzokis G, Lu PH, Tishler TA, Fong SM, Oluwadara B, Finn JP, et al. Myelin

654   breakdown and iron changes in Huntington's disease: pathogenesis and treatment

655   implications. Neurochem Res 2007;32:1655–64. https://doi.org/10.1007/s11064-007-

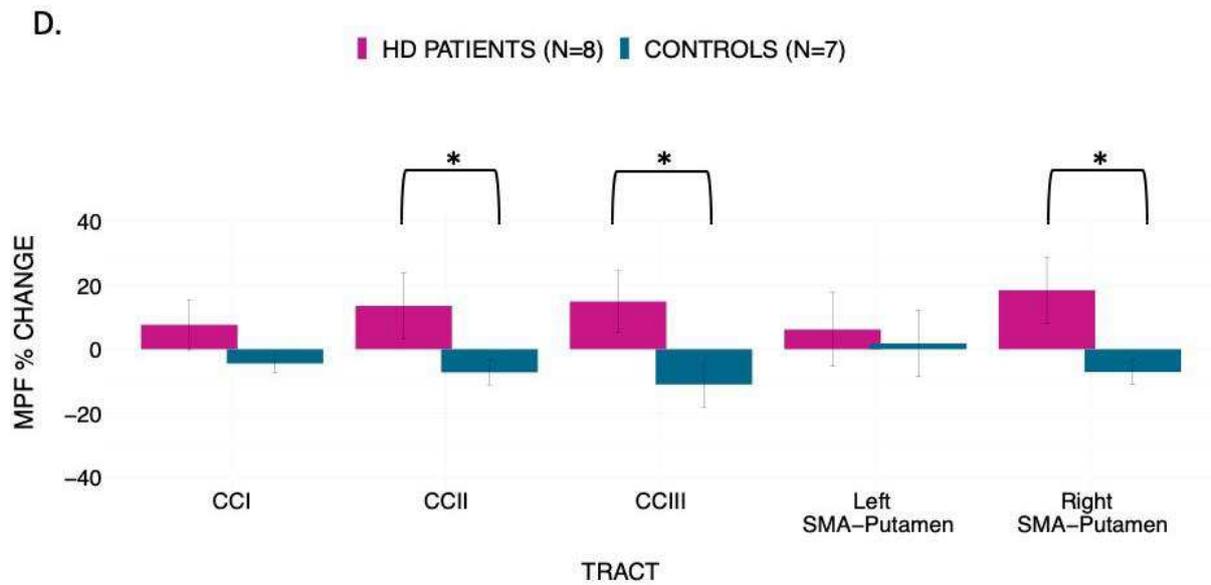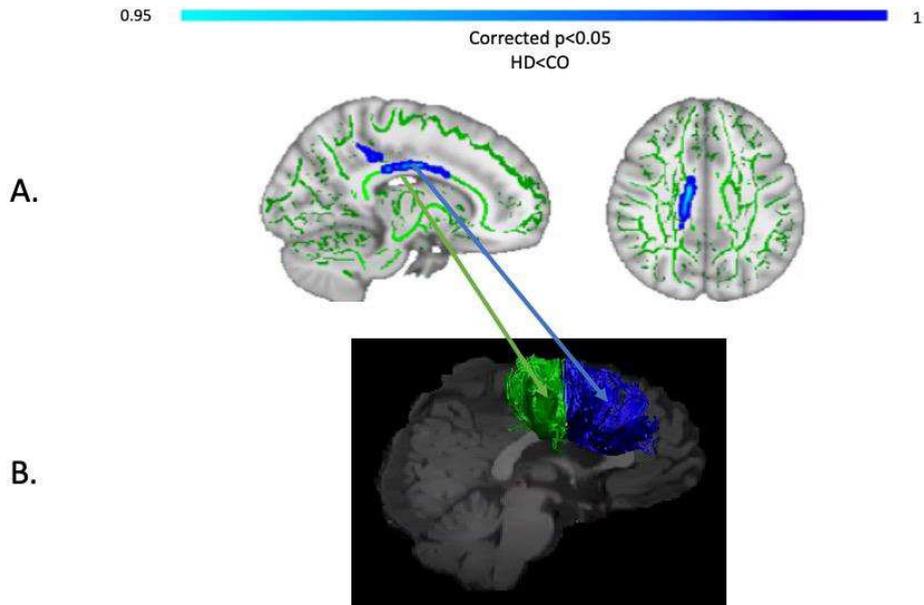656   9352-7.

657   [4]   Beglinger LJ, Langbehn DR, Duff K, Stierman L, Black DW, Nehl C, et al. Probability

658   of obsessive and compulsive symptoms in Huntington's disease. Biol Psychiatry

659   2007;61:415–8. https://doi.org/10.1016/j.biopsych.2006.04.034.

660   [5]   Ciarmiello A, Cannella M, Lastoria S, Simonelli M, Frati L, Rubinsztein DC, et al. Brain

661   white-matter volume loss and glucose hypometabolism precede the clinical symptoms

662   of Huntington's disease. J Nucl Med Off Publ Soc Nucl Med 2006;47:215–22.

663   [6]   Gregory S, Crawford H, Seunarine K, Leavitt B, Durr A, Roos RAC, et al. Natural

664   biological variation of white matter microstructure is accentuated in Huntington's

665   disease. Hum Brain Mapp 2018;39:3516–27. https://doi.org/10.1002/hbm.24191.

666   [7]   Paulsen JS, Langbehn DR, Stout JC, Aylward E, Ross CA, Nance M, et al. Detection of

667   Huntington's disease decades before diagnosis: the Predict-HD study. J Neurol

668   Neurosurg Psychiatry 2008;79:874–80. https://doi.org/10.1136/jnnp.2007.128728.

669   [8]   Rosas HD, Wilkens P, Salat DH, Mercaldo ND, Vangel M, Yendiki AY, et al. Complex

670   spatial and temporally defined myelin and axonal degeneration in Huntington disease.

671   NeuroImage Clin 2018;20:236–42. https://doi.org/10.1016/j.nicl.2018.01.029.

672   [9]   Wang N, Yang XW. Huntington Disease's Glial Progenitor Cells Hit the Pause Button in

673   the   Mouse   Brain.   Cell   Stem   Cell   2019;24:3–4.

674   https://doi.org/10.1016/j.stem.2018.12.004.

675   [10]   Gómez-Tortosa E, MacDonald ME, Friend JC, Taylor SA, Weiler LJ, Cupples LA, et al.

676   Quantitative neuropathological changes in presymptomatic Huntington's disease. Ann

677   Neurol 2001;49:29–34.

678   [11]   Huang B, Wei W, Wang G, Gaertig MA, Feng Y, Wang W, et al. Mutant huntingtin

679   downregulates myelin regulatory factor-mediated myelin gene expression and affects

680   mature   oligodendrocytes.   Neuron   2015;85:1212–26.

681   https://doi.org/10.1016/j.neuron.2015.02.026.

682   [12]   Jin J, Peng Q, Hou Z, Jiang M, Wang X, Langseth AJ, et al. Early white matter

683   abnormalities, progressive brain pathology and motor deficits in a novel knock-in mouse

684   model   of   Huntington's   disease.   Hum   Mol   Genet   2015;24:2508–27.

685   https://doi.org/10.1093/hmg/ddv016.

686   [13]   Myers RH, Vonsattel JP, Paskevich PA, Kiely DK, Stevens TJ, Cupples LA, et al.

687   Decreased Neuronal and Increased Oligodendroglial Densities in Huntington's Disease

688   Caudate   Nucleus.   J   Neuropathol   Exp   Neurol   1991;50:729–42.

689   https://doi.org/10.1097/00005072-199111000-00005.

690   [14]   Simmons DA, Casale M, Alcon B, Pham N, Narayan N, Lynch G. Ferritin accumulation

691   in dystrophic microglia is an early event in the development of Huntington's disease.

692   Glia n.d.;55:1074–84. https://doi.org/10.1002/glia.20526.

693 [15] Teo RTY, Hong X, Yu-Taeger L, Huang Y, Tan LJ, Xie Y, et al. Structural and molecular

694   myelination deficits occur prior to neuronal loss in the YAC128 and BACHD models of

695   Huntington   disease.   Hum   Mol   Genet   2016;25:2621–32.

696   https://doi.org/10.1093/hmg/ddw122.

697 [16] Martenson RE. Myelin. CRC Press; 1992.

698 [17] Han I, You Y, Kordower JH, Brady ST, Morfini GA. Differential vulnerability of neurons

699   in Huntington's disease: the role of cell type-specific features. J Neurochem

700   2010;113:1073–91. https://doi.org/10.1111/j.1471-4159.2010.06672.x.

701 [18] Barker R, Mason SL. The hunt for better treatments for Huntington's disease. Lancet

702   Neurol 2019;18:131–3. https://doi.org/10.1016/S1474-4422(18)30448-4.

703 [19] Shannon KM. Recent Advances in the Treatment of Huntington's Disease: Targeting

704   DNA and RNA. CNS Drugs 2020;34:219–28. https://doi.org/10.1007/s40263-019-

705   00695-3.

706 [20] Wood NI, Glynn D, Morton AJ. "Brain training" improves cognitive performance and

707   survival in a transgenic mouse model of Huntington's disease. Neurobiol Dis

708   2011;42:427–37. https://doi.org/10.1016/j.nbd.2011.02.005.

709 [21] Yhnell E, Lelos MJ, Dunnett SB, Brooks SP. Cognitive training modifies disease

710   symptoms in a mouse model of Huntington's disease. Exp Neurol 2016;282:19–26.

711   https://doi.org/10.1016/j.expneurol.2016.05.008.

712 [22] Yhnell E, Furby H, Breen RS, Brookes-Howell LC, Drew CJG, Playle R, et al. Exploring

713   computerised cognitive training as a therapeutic intervention for people with

714   Huntington's disease (CogTrainHD): protocol for a randomised feasibility study. Pilot

715   Feasibility Stud 2018;4:45. https://doi.org/10.1186/s40814-018-0237-0.

716 [23] Caeyenberghs K, Metzler-Baddeley C, Foley S, Jones DK. Dynamics of the Human
717   Structural Connectome Underlying Working Memory Training. J Neurosci Off J Soc
718   Neurosci 2016;36:4056–66. https://doi.org/10.1523/JNEUROSCI.1973-15.2016.

719 [24] Taubert M, Lohmann G, Margulies DS, Villringer A, Ragert P. Long-term effects of
720   motor training on resting-state networks and underlying brain structure. NeuroImage
721   2011;57:1492–8. https://doi.org/10.1016/j.neuroimage.2011.05.078.

722 [25] Metzler-Baddeley C, Cantera J, Coulthard E, Rosser A, Jones DK, Baddeley RJ.
723   Improved Executive Function and Callosal White Matter Microstructure after Rhythm
724   Exercise   in   Huntington's   Disease.   J   Huntingt   Dis   2014;3:273–83.
725   https://doi.org/10.3233/JHD-140113.

726 [26] Drijkoningen D, Caeyenberghs K, Leunissen I, Vander Linden C, Leemans A, Sunaert S,
727   et al. Training-induced improvements in postural control are accompanied by alterations
728   in cerebellar white matter in brain injured patients. NeuroImage Clin 2014;7:240–51.
729   https://doi.org/10.1016/j.nicl.2014.12.006.

730 [27] Scholz J, Klein MC, Behrens TEJ, Johansen-Berg H. Training induces changes in white
731   matter architecture. Nat Neurosci 2009;12:1370–1. https://doi.org/10.1038/nn.2412.

732 [28] Hu Y, Geng F, Tao L, Hu N, Du F, Fu K, et al. Enhanced white matter tracts integrity in
733   children   with   abacus   training.   Hum   Brain   Mapp   2011;32:10–21.
734   https://doi.org/10.1002/hbm.20996.

735 [29] Bengtsson SL, Nagy Z, Skare S, Forsman L, Forssberg H, Ullén F. Extensive piano
736   practicing has regionally specific effects on white matter development. Nat Neurosci
737   2005;8:1148–50. https://doi.org/10.1038/nn1516.

738 [30] Han Y, Yang H, Lv Y-T, Zhu C-Z, He Y, Tang H-H, et al. Gray matter density and white
739   matter integrity in pianists' brain: A combined structural and diffusion tensor MRI study.
740   Neurosci Lett 2009;459:3–6. https://doi.org/10.1016/j.neulet.2008.07.056.

741   [31] Takeuchi H, Sekiguchi A, Taki Y, Yokoyama S, Yomogida Y, Komuro N, et al. Training

742   of working memory impacts structural connectivity. J Neurosci Off J Soc Neurosci

743   2010;30:3297–303. https://doi.org/10.1523/JNEUROSCI.4611-09.2010.

744   [32] Mackey A, Whitaker K, Bunge S. Experience-dependent plasticity in white matter

745   microstructure: reasoning training alters structural connectivity. Front Neuroanat

746   2012;6:32. https://doi.org/10.3389/fnana.2012.00032.

747   [33] Tang Y-Y, Lu Q, Fan M, Yang Y, Posner MI. Mechanisms of white matter changes

748   induced   by   meditation.   Proc   Natl   Acad   Sci   2012;109:10570–4.

749   https://doi.org/10.1073/pnas.1207817109.

750   [34] Caeyenberghs K, Clemente A, Imms P, Egan G, Hocking DR, Leemans A, et al. Evidence

751   for Training-Dependent Structural Neuroplasticity in Brain-Injured Patients: A Critical

752   Review.   Neurorehabil   Neural   Repair   2018;32:99–114.

753   https://doi.org/10.1177/1545968317753076.

754   [35] Gibson EM, Purger D, Mount CW, Goldstein AK, Lin GL, Wood LS, et al. Neuronal

755   Activity Promotes Oligodendrogenesis and Adaptive Myelination in the Mammalian

756   Brain. Science 2014;344:1252304. https://doi.org/10.1126/science.1252304.

757   [36] Mensch S, Baraban M, Almeida R, Czopka T, Ausborn J, El Manira A, et al. Synaptic

758   vesicle release regulates myelin sheath number of individual oligodendrocytes in vivo.

759   Nat Neurosci 2015;18:628–30. https://doi.org/10.1038/nn.3991.

760   [37] Sampaio-Baptista C, Khrapitchev AA, Foxley S, Schlagheck T, Scholz J, Jbabdi S, et al.

761   Motor Skill Learning Induces Changes in White Matter Microstructure and Myelination.

762   J Neurosci 2013;33:19499–503. https://doi.org/10.1523/JNEUROSCI.3048-13.2013.

763   [38] Lakhani B, Borich MR, Jackson JN, Wadden KP, Peters S, Villamayor A, et al. Motor

764   Skill   Acquisition   Promotes   Human   Brain   Myelin   Plasticity.   Neural   Plast

765   2016;2016:7526135. https://doi.org/10.1155/2016/7526135.

766 [39] Costa RM, Cohen D, Nicolelis MAL. Differential corticostriatal plasticity during fast and

767   slow motor skill learning in mice. Curr Biol CB 2004;14:1124–34.

768   https://doi.org/10.1016/j.cub.2004.06.053.

769 [40] Shmuelof L, Krakauer JW. Are we ready for a natural history of motor learning? Neuron

770   2011;72:469–76. https://doi.org/10.1016/j.neuron.2011.10.017.

771 [41] Steele CJ, Bailey JA, Zatorre RJ, Penhune VB. Early musical training and white-matter

772   plasticity in the corpus callosum: evidence for a sensitive period. J Neurosci Off J Soc

773   Neurosci 2013;33:1282–90. https://doi.org/10.1523/JNEUROSCI.3578-12.2013.

774 [42] Yin HH, Mulcare SP, Hilário MRF, Clouse E, Holloway T, Davis MI, et al. Dynamic

775   reorganization of striatal circuits during the acquisition and consolidation of a skill. Nat

776   Neurosci 2009;12:333–41. https://doi.org/10.1038/nn.2261.

777 [43] Sagi Y, Tavor I, Hofstetter S, Tzur-Moryosef S, Blumenfeld-Katzir T, Assaf Y. Learning

778   in the Fast Lane: New Insights into Neuroplasticity. Neuron 2012;73:1195–203.

779   https://doi.org/10.1016/j.neuron.2012.01.025.

780 [44] Xiao L, Ohayon D, McKenzie IA, Sinclair-Wilson A, Wright JL, Fudge AD, et al. Rapid

781   production of new oligodendrocytes is required in the earliest stages of motor skill

782   learning. Nat Neurosci 2016;19:1210–7. https://doi.org/10.1038/nn.4351.

783 [45] Papoutsi M, Labuschagne I, Tabrizi SJ, Stout JC. The cognitive burden in Huntington's

784   disease: Pathology, phenotype, and mechanisms of compensation. Mov Disord

785   2014;29:673–83. https://doi.org/10.1002/mds.25864.

786 [46] Nakamura T, Nagata M, Yagi T, Graybiel AM, Yamamori T, Kitsukawa T. Learning new

787   sequential stepping patterns requires striatal plasticity during the earliest phase of

788   acquisition. Eur J Neurosci 2017;45:901–11. https://doi.org/10.1111/ejn.13537.

789 [47] Lanciego JL, Luquin N, Obeso JA. Functional neuroanatomy of the basal ganglia. Cold

790   Spring   Harb   Perspect   Med   2012;2:a009621–a009621.

791   https://doi.org/10.1101/cshperspect.a009621.

792 [48] Guitar NA, Connelly DM, Nagamatsu LS, Orange JB, Muir-Hunter SW. The effects of

793   physical exercise on executive function in community-dwelling older adults living with

794   Alzheimer's-type dementia: A systematic review. Ageing Res Rev 2018;47:159–67.

795   https://doi.org/10.1016/j.arr.2018.07.009.

796 [49] Duchesne C, Lungu O, Nadeau A, Robillard ME, Boré A, Bobeuf F, et al. Enhancing both

797   motor and cognitive functioning in Parkinson's disease: Aerobic exercise as a

798   rehabilitative   intervention.   Brain   Cogn   2015;99:68–77.

799   https://doi.org/10.1016/j.bandc.2015.07.005.

800 [50] Giacosa C, Karpati FJ, Foster NEV, Penhune VB, Hyde KL. Dance and music training

801   have different effects on white matter diffusivity in sensorimotor pathways. NeuroImage

802   2016;135:273–86. https://doi.org/10.1016/j.neuroimage.2016.04.048.

803 [51] Pierpaoli C, Basser PJ. Toward a quantitative assessment of diffusion anisotropy. Magn

804   Reson Med 1996;36:893–906.

805 [52] De Santis S, Drakesmith M, Bells S, Assaf Y, Jones DK. Why diffusion tensor MRI does

806   well only some of the time: Variance and covariance of white matter tissue

807   microstructure attributes in the living human brain. Neuroimage 2014;89:35–44.

808   https://doi.org/10.1016/j.neuroimage.2013.12.003.

809 [53] Wheeler-Kingshott CAM, Cercignani M. About "axial" and "radial" diffusivities. Magn

810   Reson Med 2009;61:1255–60. https://doi.org/10.1002/mrm.21965.

811 [54] Sled JG. Modelling and interpretation of magnetization transfer imaging in the brain.

812   NeuroImage 2018;182:128–35. https://doi.org/10.1016/j.neuroimage.2017.11.065.

813   [55] Assaf Y, Basser PJ. Composite hindered and restricted model of diffusion (CHARMED)

814   MR   imaging   of   the   human   brain.   NeuroImage   2005;27:48–58.

815   https://doi.org/10.1016/j.neuroimage.2005.03.042.

816   [56] Lövdén M, Bodammer NC, Kühn S, Kaufmann J, Schütze H, Tempelmann C, et al.

817   Experience-dependent plasticity of white-matter microstructure extends into old age.

818   Neuropsychologia   2010;48:3878–83.

819   https://doi.org/10.1016/j.neuropsychologia.2010.08.026.

820   [57] Zatorre RJ, Fields RD, Johansen-Berg H. Plasticity in gray and white: neuroimaging

821   changes   in   brain   structure   during   learning.   Nat   Neurosci   2012;15:528–36.

822   https://doi.org/10.1038/nn.3045.

823   [58] Serres S, Anthony DC, Jiang Y, Campbell SJ, Broom KA, Khrapitchev A, et al.

824   Comparison of MRI signatures in pattern I and II multiple sclerosis models. NMR

825   Biomed 2009;22:1014–24. https://doi.org/10.1002/nbm.1404.

826   [59] Ou X, Sun S-W, Liang H-F, Song S-K, Gochberg DF. The MT pool size ratio and the

827   DTI radial diffusivity may reflect the myelination in shiverer and control mice. NMR

828   Biomed 2009;22:480–7. https://doi.org/10.1002/nbm.1358.

829   [60] Levesque IR, Giacomini PS, Narayanan S, Ribeiro LT, Sled JG, Arnold DL, et al.

830   Quantitative magnetization transfer and myelin water imaging of the evolution of acute

831   multiple   sclerosis   lesions.   Magn   Reson   Med   2010;63:633–40.

832   https://doi.org/10.1002/mrm.22244.

833   [61] Schmierer K, Tozer DJ, Scaravilli F, Altmann DR, Barker GJ, Tofts PS, et al. Quantitative

834   Magnetization Transfer Imaging in Postmortem Multiple Sclerosis Brain. J Magn Reson

835   Imaging JMRI 2007;26:41–51. https://doi.org/10.1002/jmri.20984.

836 [62] Barazany D, Basser PJ, Assaf Y. In vivo measurement of axon diameter distribution in

837   the corpus callosum of rat brain. Brain 2009;132:1210–20.

838   https://doi.org/10.1093/brain/awp042.

839 [63] Poudel GR, Stout JC, Domínguez D JF, Salmon L, Churchyard A, Chua P, et al. White

840   matter connectivity reflects clinical and cognitive status in Huntington's disease.

841   Neurobiol Dis 2014;65:180–7. https://doi.org/10.1016/j.nbd.2014.01.013.

842 [64] Hofer S, Frahm J. Topography of the human corpus callosum revisited--comprehensive

843   fiber tractography using diffusion tensor magnetic resonance imaging. NeuroImage

844   2006;32:989–94. https://doi.org/10.1016/j.neuroimage.2006.05.044.

845 [65] Vonsattel JPG, Difiglia M. Huntington Disease. J Neuropathol Exp Neurol 1998;57:369–

846   84. https://doi.org/10.1097/00005072-199805000-00001.

847 [66] Diana Rosas H, Lee SY, Bender A, Zaleta AK, Vange M, Yu P, et al. Altered White

848   Matter Microstructure in the Corpus Callosum in Huntington's Disease: implications for

849   cortical "disconnection." NeuroImage 2010;49:2995–3004.

850   https://doi.org/10.1016/j.neuroimage.2009.10.015.

851 [67] Phillips O, Sanchez-Castaneda C, Elifani F, Maglione V, Pardo AD, Caltagirone C, et al.

852   Tractography of the Corpus Callosum in Huntington's Disease. PLOS ONE

853   2013;8:e73280. https://doi.org/10.1371/journal.pone.0073280.

854 [68] Dumas EM, van den Bogaard SJA, Ruber ME, Reilman RR, Stout JC, Craufurd D, et al.

855   Early changes in white matter pathways of the sensorimotor cortex in premanifest

856   Huntington's disease. Hum Brain Mapp 2012;33:203–12.

857   https://doi.org/10.1002/hbm.21205.

858 [69] Bourbon-Teles J, Bells S, Jones DK, Coulthard E, Rosser A, Metzler-Baddeley C. Myelin

859   Breakdown in Human Huntington's Disease: Multi-Modal Evidence from Diffusion

860   MRI and Quantitative Magnetization Transfer. Non-Invasive MRI Window Brain

861   Inflamm 2019;403:79–92. https://doi.org/10.1016/j.neuroscience.2017.05.042.

862 [70] Smith SM, Jenkinson M, Johansen-Berg H, Rueckert D, Nichols TE, Mackay CE, et al.

863   Tract-based spatial statistics: Voxelwise analysis of multi-subject diffusion data.

864   NeuroImage 2006;31:1487–505. https://doi.org/10.1016/j.neuroimage.2006.02.024.

865 [71] Nasreddine ZS, Phillips NA, Bédirian V, Charbonneau S, Whitehead V, Collin I, et al.

866   The Montreal Cognitive Assessment, MoCA: A Brief Screening Tool For Mild

867   Cognitive Impairment. J Am Geriatr Soc 2005;53:695–9. https://doi.org/10.1111/j.1532-

868   5415.2005.53221.x.

869 [72] Nelson H. National Adult Reading Test (NART) test manual (Part 1 n.d.

870 [73] Baddeley A. Exploring the central executive. Q J Exp Psychol A 1996;49A:5–28.

871   https://doi.org/10.1080/027249896392784.

872 [74] Baldo JV, Shimamura AP, Delis DC, Kramer J, Kaplan E. Verbal and design fluency in

873   patients with frontal lobe lesions. J Int Neuropsychol Soc 2001;7:586–96.

874   https://doi.org/10.1017/S1355617701755063.

875 [75] Jones DK, Horsfield MA, Simmons A. Optimal strategies for measuring diffusion in

876   anisotropic systems by magnetic resonance imaging. Magn Reson Med 1999;42:515–

877   25.

878 [76] Cercignani M, Alexander DC. Optimal acquisition schemes for in vivo quantitative

879   magnetization transfer MRI. Magn Reson Med 2006;56:803–10.

880   https://doi.org/10.1002/mrm.21003.

881 [77] Irfanoglu MO, Walker L, Sarlls J, Marenco S, Pierpaoli C. Effects of image distortions

882   originating from susceptibility variations and concomitant fields on diffusion MRI

883   tractography results. NeuroImage 2012;61:275–88.

884   https://doi.org/10.1016/j.neuroimage.2012.02.054.

885   [78] Leemans A, Jones DK. The B-matrix must be rotated when correcting for subject motion

886   in DTI data. Magn Reson Med 2009;61:1336–49. https://doi.org/10.1002/mrm.21890.

887   [79] Leemans A, Jeurissen B, Sijbers J, Jones D. ExploreDTI: a graphical toolbox for

888   processing, analyzing, and visualizing diffusion MR data. Proc Intl Soc Mag Reson Med,

889   vol. 17, 2009.

890   [80] Pasternak O, Sochen N, Gur Y, Intrator N, Assaf Y. Free water elimination and mapping

891   from   diffusion   MRI.   Magn   Reson   Med   2009;62:717–30.

892   https://doi.org/10.1002/mrm.22055.

893   [81] Ben-Amitay S, Jones DK, Assaf Y. Motion correction and registration of high b-value

894   diffusion   weighted   images.   Magn   Reson   Med   2012;67:1694–702.

895   https://doi.org/10.1002/mrm.23186.

896   [82] Klein S, Staring M, Murphy K, Viergever MA, Pluim JPW. elastix: a toolbox for

897   intensity-based medical image registration. IEEE Trans Med Imaging 2010;29:196–205.

898   https://doi.org/10.1109/TMI.2009.2035616.

899   [83] Henkelman RM, Huang X, Xiang QS, Stanisz GJ, Swanson SD, Bronskill MJ.

900   Quantitative interpretation of magnetization transfer. Magn Reson Med 1993;29:759–

901   66.

902   [84] Ramani A, Dalton C, Miller DH, Tofts PS, Barker GJ. Precise estimate of fundamental

903   in-vivo MT parameters in human brain in clinically feasible times. Magn Reson Imaging

904   2002;20:721–31. https://doi.org/10.1016/S0730-725X(02)00598-2.

905   [85] Dell'acqua F, Scifo P, Rizzo G, Catani M, Simmons A, Scotti G, et al. A modified damped

906   Richardson-Lucy   algorithm   to   reduce   isotropic   background   effects   in   spherical

907   deconvolution.   NeuroImage   2010;49:1446–58.

908   https://doi.org/10.1016/j.neuroimage.2009.09.033.

909   [86] Jeurissen B, Leemans A, Jones DK, Tournier J-D, Sijbers J. Probabilistic fiber tracking

910   using the residual bootstrap with constrained spherical deconvolution. Hum Brain Mapp

911   2011;32:461–79. https://doi.org/10.1002/hbm.21032.

912   [87] Catani M, Howard RJ, Pajevic S, Jones DK. Virtual in vivo interactive dissection of white

913   matter   fasciculi   in   the   human   brain.   NeuroImage   2002;17:77–94.

914   https://doi.org/10.1006/nimg.2002.1136.

915   [88] Leh SE, Ptito A, Chakravarty MM, Strafella AP. Fronto-striatal connections in the human

916   brain: a probabilistic diffusion tractography study. Neurosci Lett 2007;419:113–8.

917   https://doi.org/10.1016/j.neulet.2007.04.049.

918   [89] Mair P, Wilcox R. Robust statistical methods in R using the WRS2 package. Behav Res

919   Methods 2020;52:464–88. https://doi.org/10.3758/s13428-019-01246-w.

920   [90] Wilcox RR. Introduction to robust estimation and hypothesis testing. Academic press;

921   2011.

922   [91] Testa R, Bennett P, Ponsford J. Factor analysis of nineteen executive function tests in a

923   healthy adult population. Arch Clin Neuropsychol Off J Natl Acad Neuropsychol

924   2012;27:213–24. https://doi.org/10.1093/arclin/acr112.

925   [92] Preacher KJ, MacCallum RC. Exploratory Factor Analysis in Behavior Genetics

926   Research: Factor Recovery with Small Sample Sizes. Behav Genet 2002;32:153–61.

927   https://doi.org/10.1023/A:1015210025234.

928   [93] Winter* JCF de, Dodou* D, Wieringa PA. Exploratory Factor Analysis With Small

929   Sample   Sizes.   Multivar   Behav   Res   2009;44:147–81.

930   https://doi.org/10.1080/00273170902794206.

931   [94] Cattell RB. The Scree Test For The Number Of Factors. Multivar Behav Res 1966;1:245–

932   76. https://doi.org/10.1207/s15327906mbr0102_10.

933   [95] Cohen J. Statistical power analysis for the behavioral sciences. Academic press; 2013.

934   [96] Benjamini Y, Hochberg Y. Controlling the False Discovery Rate: A Practical and

935   Powerful Approach to Multiple Testing. J R Stat Soc Ser B Methodol 1995;57:289–300.

936   [97] Penke L, Maniega SM, Murray C, Gow AJ, Hernández MCV, Clayden JD, et al. A

937   General Factor of Brain White Matter Integrity Predicts Information Processing Speed

938   in   Healthy   Older   People.   J   Neurosci   2010;30:7569–74.

939   https://doi.org/10.1523/JNEUROSCI.1553-10.2010.

940   [98] Wahl M, Li Y-O, Ng J, Lahue SC, Cooper SR, Sherr EH, et al. Microstructural

941   correlations of white matter tracts in the human brain. NeuroImage 2010;51:531–41.

942   https://doi.org/10.1016/j.neuroimage.2010.02.072.

943   [99] Westfall J, Yarkoni T. Statistically Controlling for Confounding Constructs Is Harder than

944   You   Think.   PLOS   ONE   2016;11:e0152719.

945   https://doi.org/10.1371/journal.pone.0152719.

946   [100] Henkelman RM, Stanisz GJ, Graham SJ. Magnetization transfer in MRI: a review. NMR

947   Biomed n.d.;14:57–64. https://doi.org/10.1002/nbm.683.

948   [101] Rocha NP, Ribeiro FM, Furr-Stimming E, Teixeira AL. Neuroimmunology of

949   Huntington's disease: revisiting evidence from human studies. Mediators Inflamm

950   2016;2016.

951   [102] Vinther-Jensen T, Simonsen AH, Budtz-Jørgensen E, Hjermind LE, Nielsen JE.

952   Ubiquitin: a potential cerebrospinal fluid progression marker in Huntington's disease.

953   Eur J Neurol n.d.;22:1378–84. https://doi.org/10.1111/ene.12750.

954   [103] Wang Y, van Gelderen P, de Zwart JA, Duyn JH. B0-field dependence of MRI T1

955   relaxation   in   human   brain.   NeuroImage   2020;213:116700.

956   https://doi.org/10.1016/j.neuroimage.2020.116700.

957   [104] Chomiak T, Hu B. What Is the Optimal Value of the g-Ratio for Myelinated Fibers in

958   the Rat CNS? A Theoretical Approach. PLOS ONE 2009;4:e7754.

959   https://doi.org/10.1371/journal.pone.0007754.

960   [105] Kaller MS, Lazari A, Blanco-Duque C, Sampaio-Baptista C, Johansen-Berg H. Myelin

961   plasticity and behaviour—connecting the dots. Curr Opin Neurobiol 2017;47:86–92.

962   https://doi.org/10.1016/j.conb.2017.09.014.

963   [106] Rushton WAH. A theory of the effects of fibre size in medullated nerve. J Physiol

964   1951;115:101–22.

965   [107] Valkanova V, Eguia Rodriguez R, Ebmeier KP. Mind over matter--what do we know

966   about neuroplasticity in adults? Int Psychogeriatr 2014;26:891–909.

967   https://doi.org/10.1017/S1041610213002482.

968   [108] Thomas C, Baker CI. Teaching an adult brain new tricks: A critical review of evidence

969   for training-dependent structural plasticity in humans. NeuroImage 2013;73:225–36.

970   https://doi.org/10.1016/j.neuroimage.2012.03.069.

971   [109] Trenerry MR, Crosson B, DeBoe J, Leber WR. Stroop neuropsychological screening

972   test. Odessa FL Psychol Assess Resour 1989.

973   [110] Delis DC, Kramer JH, Kaplan E, Holdnack J. Reliability and validity of the Delis-Kaplan

974   Executive Function System: an update. J Int Neuropsychol Soc JINS 2004;10:301–3.

975   https://doi.org/10.1017/S1355617704102191.

976

977

	Age	Length of CAG repeats	TMS	FAS
Mean (Range)	48.5 (22-68)	43.6 (40-51)	18.7 (0-69)	22.6 (17-25)
SD	15.6	3.5	24.7	3.3

Table 1. *Demographics and background clinical information of the patients' cohort. Based on TMS and FAS, most of the patients were at early disease stages, however two of them were more advanced. Abbreviations: CAG = cytosine-adenine-guanine; TMS = Total Motor Score out of 124 (the higher the scores the more impaired the performance); FAS = Functional Assessment Score out of 25 (the higher the scores the better the performance); SD = Standard Deviation.*

Mean (SD, range)	Patients (n = 8)	Controls (n = 9)	Mann-Whitney U (p-value)
Age	48.5 (15.62, 22-68)	52.6 (14.56, 22-68)	U = 31 (p = 0.673)
NART-IQ	106.3 (13.13, 94-123)	121.22 (4.32, 117-128)	U = 8 (p = 0.006)
MoCa	23 (5.6, 14-29)	27.67 (1, 26-29)	U = 14 (p = 0.036)

Table 2. *Demographics and general cognitive profile of patients and controls. Both groups were matched for age, sex and years of education but the patient group had a*

lower NART-IQ and performed less well than the control group in the MoCA.

Abbreviations: NART-IQ = verbal IQ estimate based on the National Adult Reading

Test; MoCA = Montreal Cognitive Assessment score out of 30.

993

994

Task	Outcome variables	Description
Simultaneous box crossing and digit sequences repetition [73]	Correct digits recalled under single task condition; correct digits recalled under dual task conditions; boxes identified under dual task condition.	Correct number of recalled digits in a standard digit span test; correct number of recalled digits in the dual condition; number of boxes identified in the dual condition
Stroop test [109]	Stroop interference score	Calculated by subtracting the number of errors from the total number of items presented in the test
Trials test [73]	Trail test switching	Performance accuracy: reflects the ability of moving flexibly from one set of rules to another in response to changing task requirements

	Verbal and category fluency	Number of generated words starting with the following letters: "F", "A", "S" and "M", "C", "R"; number of generated words belonging to the following categories: "animals" and "boys' names" and "supermarket items" and "girls' names"
Verbal and category fluency test [110]		

Table 3. Cognitive outcome variables assessed in this study. Tests were carried out
before and after the training, and a percentage change score was computed for each
variable.

	T$_1$-w	DTI	CHARMED	T1 map	MT-w	B0 map
Pulse sequence	FSPGR	SE\EPI	SE\EPI	SPGR (3D)	FSPGR (3D)	SPGR (3D)
Matrix size	256×256	96×96	96×96	96×96×60	96×96×60	128×128
FoV (mm)	230	230	230	240	240	220
Slices	172	60	60	-	-	-

Slice thickness (mm)	1	2.4	2.4	-	-	-
TE,TR (ms)	7.8, 2.9	87, 16000	126, 17000	6.85, 1.2	2.18,25.82	TE: 9 & 7 TR: 20
Off-resonance pulses (Hz/°)	-	-	-	-	100[38]0/332, 1000/333, 12062/628, 47185/628, 56363/332, 2751/628, 1000/628, 1000/628, 2768/628, 2791/628, 2887/628	-
Flip angles (°)	20	90	90	15,7,3	5	90

Table 4. Scan parameters. All sequences were acquired at 3T. For each of the sequences, the main acquisition parameters are provided. T_1-w: T_1-weighted; MT-w: MT-weighted; FSPGR: fast spoiled gradient echo; SE: spin-echo; EPI: echo-planar imaging; SPGR: spoiled gradient recalled-echo; FoV: field of view; TE: echo time; TR: repetition time.

% Change	Executive	Working memory capacity	Fluency
Total box (dual)	**0.864**	0.022	0.419
Stroop interference score	**0.811**	-0.270	-0.267
Trail test switching	**0.731**	-0.470	0.162
Correct digits under single task condition	0.201	**0.904**	0.129
Correct digits under dual task condition	-0.193	**0.855**	-0.018
Category fluency	-0.070	-0.138	**0.817**
Verbal fluency	-0.026	-0.232	**-0.799**

1009 ***Table 5.*** *Rotated Component Loadings on Change in the Cognitive Benchmark Tests.*

1010 *Significant loadings (>0.5) are highlighted in bold.*

1011

1012

FA	t	p	FDR corrected p
CCI	1.220	0.909	0.91
CCII	2.650	0.91	0.91

CCIII	0.320	0.48	0.91
Left SMA-Putamen	5.160	0.77	0.91
Right SMA-Putamen	-9.54	0.02	0.11
RD			
CCI	-0.48	0.35	0.45
CCII	-1.29	0.22	0.45
CCIII	-1.04	0.30	0.45
Left SMA-Putamen	-3.68	0.08	0.39
Right SMA-Putamen	4.010	0.80	0.80
Fr			
CCI	0.033	0.81	0.82
CCII	-0.001	0.49	0.82
CCIII	0.03	0.82	0.82
Left SMA-Putamen	0.01	0.58	0.82
Right SMA-Putamen	-0.052	0.1996	0.817
MPF			
CCI	-12.06	0.08	0.10
CCII	-20.72	0.03	**0.05**

CCIII	-25.87	0.02	**0.05**
Left SMA-Putamen	-4.34	0.38	0.38
Right SMA-Putamen	-25.48	0.02	**0.05**

1013 ***Table 6.*** *Summary statistics for the permutation analysis of training effects on FA, RD,*

1014 *Fr and MPF, across the investigated tracts.*

1015

1016

1017

1018

1019 ***Figure 1.*** (1) ***pathway regions of interest.*** *Sagittal views of the reconstructed WM*

1020 *pathways displayed on a T_1-weighted image for one control participant. (A) CCI, CCII,*

1021 *and CCIII (Hofer and Frahm, 2006): CCI is the most anterior portion of the CC and*

1022 *maintains prefrontal connections between both hemispheres; CCII is the portion that*

1023 *maintains connections between premotor and supplementary motor areas of both*

1024 *hemispheres. CCIII maintains connections between primary motor cortices of both*

1025 *hemispheres. (B) SMA-putamen pathway: this pathway has efferent and afferent*

1026 *projections to the primary motor cortex and is involved in movement execution.*

1027

1028 ***Figure 2. Sagittal views of the tractography protocols.*** *(A) CCI, CCII and CCIII (B)*

1029 *SMA - putamen pathway. Booleian logic OR waypoint regions of interest gates are*

1030 *illustrated in blue; AND gates in green. M = Midline.*

1031

1032 ***Figure 3.*** *Correlation matrices for the MRI metrics investigated across the different*

1033 *WM pathways. Colour intensity and the size of the circles are proportional to the*

strength of the correlation. * p < 0.05, ** p < 0.01, *** p < 0.001. The absolute correlation coefficient is plotted. MPF values were highly correlated across tracts, whereas this was not true for the other metrics

Figure 4. Mean ratings for drumming performance *according to the Trinity College London marking criteria for percussion (2016) as a function of group and time point. Patients improved their drumming performance significantly for the easy test pattern and controls for the medium difficult test pattern. * p < 0.05, ** p < 0.01, bootstrapping based on 1000 samples.*

Figure 5. MPF changes scores*: PCA scree plot (A); plot summarising how each variable is accounted for in every principal component - colour intensity and the size of the circles are proportional to the loading: PC1 loads on CCI, CCII, CCIII and right SMA-Putamen, while PC2 loads mostly on the left SMA-Putamen; the absolute correlation coefficient is plotted (B); correlation circle, interpreted as follows: 1) positively correlated variables are grouped together, 2) negatively correlated variables are positioned on opposite sides of the plot origin (opposite quadrants), 3) the distance between variables and the origin measures the quality of the variable on the factor map. Variables that are away from the origin are well represented on the factor map (C); Bar graph of the percentage change in MPF across the inspected tracts; Error bars represent the standard error; training was associated with a significantly greater change in MPF in CCII, CCIII, and right SMA-Putamen; * (p<0.05), results corrected for multiple comparisons with FDR (D).*

1058 *Figure 6. TBSS analysis of baseline MPF values (A).* Light blue areas show a

1059 significant reduction of MPF in patients with HD compared to controls (p < 0.05, FWE

1060 corrected). The midbody of the CC was mostly found to be affected, which carries

1061 connections to the premotor, supplementary motor and motor areas of the brain.

1062 *Tracts showing significantly greater MPF changes in HD patients post-training*

1063 *as compared to controls (B).* Areas showing significant MPF reductions at baseline

1064 overlap with tracts showing significant changes post-training (i.e. CCII and CCIII).

1065

1066

1067

1068